Available online at www.sciencedirect.com

ScienceDirect

Ceramics International 40 (2014) 109–115

CERAMICS INTERNATIONAL

www.elsevier.com/locate/ceramint

Fabrication and gas sensing properties of C-doped and un-doped TiO_2 nanotubes

Necmettin Kılınç[a,b,*], Erdem Şennik[a], Müge Işık[a], Ali Şems Ahsen[a], Osman Öztürk[a], Zafer Ziya Öztürk[a,c]

[a]Department of Physics, Science Faculty, Gebze Institute of Technology, 41400 Gebze, Kocaeli, Turkey
[b]Department of Electrical and Electronics Engineering, Koc University, 34450 Sariyer, Istanbul, Turkey
[c]TÜBİTAK, Marmara Research Center, Materials Institute, 41470 Gebze, Kocaeli, Turkey

Received 7 December 2012; received in revised form 29 May 2013; accepted 29 May 2013
Available online 5 June 2013

Abstract

In this work, un-doped and carbon (C) doped TiO_2 nanotubes were fabricated and their hydrogen sensing properties were investigated. A Ti foil was anodized in an aqueous hydrofluoric acid (HF) electrolyte (0.5 wt%) at room temperature to form TiO_2 nanotube arrays. C-doped TiO_2 nanotubes were obtained through two methods; a chemical process and thermal acetylene (C_2H_2) treatment. In the chemical method, a Ti foil was anodized 'in-situ' in aqueous solution of 0.5 wt% polyvinyl alcohol (PVA)+0.5 wt% HF. In the heat treatment method, a Ti foil was anodized in an aqueous (HF) electrolyte (0.5 wt%) to obtain TiO_2 nanotubes, and then C-doped TiO_2 nanotubes were obtained by heating as-prepared nanotubes at 500 °C in a quartz tube under a continuous N_2 and C_2H_2 flux (1:1). The obtained un-doped and C-doped TiO_2 nanotubes were characterized by scanning electron microscopy (SEM), energy dispersive X-ray analysis (EDX) and X-ray photoelectron spectroscopy (XPS). The H_2 sensing properties of the nanotubes exposed to 5000 ppm H_2 were investigated at 100 °C. C-doped TiO_2 nanotubes showed a lower response to H_2 than the undoped TiO_2 nanotubes.

Keywords: TiO_2 nanotubes; Anodization; Carbon doped; H_2 sensor; Gas sensor

1. Introduction

TiO_2 nanotube arrays have been used in a wide range of application areas such as photo electrochemical materials, dye-sensitized solar cells [DSSC], hydrogen (H_2) sensors, oxygen (O_2) sensors, bio-sensing and biomedical applications, and catalyst support [1–6]. Anodic porous TiO_2 and TiO_2 nanotubes were first synthesized using hydrofluoric acid (HF) electrolyte by Zwilling et al. [7] and Gong et al. [8] respectively. Thereafter, many studies succeeded in controlling and extending nanotube morphology, length, pore size, and wall thickness [1–5]. TiO_2 nanotubes were doped with various non-metal elements such as carbon [9], nitrogen [10], and boron [11], and metal elements such as zinc [12], chromium [13], cobalt [14], silver [15], tin [16], and iron [17] for band gap engineering. In general, the doping of TiO_2 nanotubes has been investigated, in particular for photocatalytic and photovoltaic applications.

Many investigations have been performed on the hydrogen gas sensing properties of TiO_2 nanotube arrays, especially at room temperature, and the results showed that they have excellent response to hydrogen [1–6,18–25]. To improve the sensor parameters such as the sensitivity, the response time, and the recovery time and to reduce the optimal working temperature, researchers have been focused on doping of TiO_2 nanotubes and other TiO_2 nanostructures with different types of elements. There are a limited number of investigations about the gas sensing properties of doped TiO_2 nanostructures in the literature. Liu et al. recently investigated hydrogen sensing with Nb-doped TiO_2 nanotubes prepared by the anodization of TiNb alloy, and found that the Nb-doped nanotubes demonstrated a good sensitivity for the wide-range detection of both dilute and high-concentration hydrogen atmospheres ranging

*Corresponding author at: Gebze Institute of Technology, Science Faculty, Department of Physics, P.O. Box 141, 41400 Gebze, Kocaeli, Turkey. Tel.: +90 2626051333; fax: +90 262 6538490.
E-mail address: nkilinc@gyte.edu.tr (N. Kılınç).

0272-8842/$ - see front matter © 2013 Elsevier Ltd and Techna Group S.r.l. All rights reserved.
http://dx.doi.org/10.1016/j.ceramint.2013.05.110

from 50 ppm to 2% H_2 [25]. Wang et al. described nitrogen-doped TiO_2 nanotubes film for humidity sensor that had good thermal stability [26]. They fabricated N-doped TiO_2 nanotubes in order of following processes; Ti foil were anodized to form TiO_2 nanotubes, and the synthesized TiO_2 nanotubes were immersed in ammonia for 24 h, and then annealed at the temperature of 600 °C for 2 h in a nitrogen atmosphere. Mardare et al. prepared Pd-doped TiO_2 thin films (0.5 wt%) using the sol–gel technique (dip coating) on glass and silicon substrates and observed an increase in the sensitivity of TiO_2 films with Pd doping [27]. Li et al. reported a highly sensitive and stable humidity nanosensor based on LiCl doped TiO_2 nanofibers, which had large scale product uniformity with the fiber diameters ranging from 150 to 260 nm, through electrospinning and calcination techniques [28]. Moon et al. synthesized Pd-doped TiO_2 nanofibers by electrospinning, and investigated the NO_2 gas sensing properties of the nanofibers [29]. They found that a Pd-doped TiO_2 nanofiber sensor shows considerable enhancement in the NO_2 sensitivity and a lower working temperature compared to a pristine TiO_2 nanofiber sensor.

C-doped TiO_2 nanotubes have been fabricated with various methods [5,9,30–35] and used for optical applications in general. Park et al. reported fabrication of C-doped TiO_2 nanotubes [9]. After anodizing, the TiO_2 nanotubes were annealed at 450 °C in oxygen for 1 h. The nanotubes were subsequently annealed at high temperatures (500–800 °C) under a controlled CO gas flow to produce C-doped nanotubes [9]. They observed no significant morphological changes, and the doping concentration of carbon in the TiO_2 nanotube array could be controlled between 8% and 42%, depending on annealing temperature under the CO flux [9]. Hu et al. incorporated C into TiO_2 nanotubes by annealing the as-formed nanotubes in a continuous flow of Ar and acetylene gases, and then investigated the photocatalytic activity by evaluating the photo degradation of aqueous methyl blue under sunlight illumination [30]. Hahn et al. performed carbon doping by annealing the TiO_2 nanotubes in N_2 and an acetylene gas mixture at 500 °C [31]. Xu et al. pursued the carbon doping of TiO_2 nanotubes by annealing them in air at 500 °C for 1 h, and using natural gas flame oxidation at 820 °C for 18 min [32]. They found no significant change in their quantum efficiency over the visible range. Mazare et al. investigated the effect of flame annealing on the water-splitting properties of TiO_2 nanotubes that prepared with anodization method [36]. They found that flame annealed nanotubes showed a two-fold increase in the maximum water-splitting efficiency under standard AM 1.5 conditions compared to classic annealing treatments and the high efficiency was mainly explained with higher rutile content in the tube walls without a thermal degradation of the tube morphology and carbon doping had a minor contribution to the high efficiency. In addition, they studied the modification of TiO_2 nanotubes by flame annealing depending on anodization electrolyte, tube length, tube diameter and flame annealing parameters and investigated photoelectrochemical properties of the modified TiO_2 nanotubes [37]. The gas sensing properties of C-doped TiO_2 nanotubes has not been investigated yet.

In this study, C-doped TiO_2 nanotubes were prepared by the wet chemical method and heat acetylene treatment. The H_2 sensing properties of un-doped and C-doped TiO_2 nanotubes were investigated at 100 °C.

2. Experimental details

Pristine TiO_2 nanotubes were synthesized in an aqueous electrolyte of 0.5 wt% HF with a constant anodization voltage of 20 V for 45 min. Pre-cleaned Ti foil was anodized using a dc power supply and a platinum foil as the cathode in a thermo-stated bath at a temperature of 20 °C. In order to fabricate C-doped TiO_2 nanotube with the chemical method, pre-cleaned Ti foil was anodized in-situ in an aqueous electrolyte containing polyvinyl alcohol (PVA, 0.5 wt%) and HF (0.5 wt%) by using same conditions that used for synthesizing the un-doped TiO_2 nanotubes. All solutions were prepared from reagent grade chemicals and deionized water (18 MΩ). Before the anodization experiments, the solutions were stirred using a magnetic stirrer. After the anodization, the samples were rinsed in deionized water and then dried. All samples were annealed under dry air flow at a temperature of 500 °C for 3 h to obtain crystallized TiO_2 with both anatase and rutile phases. In addition, the following procedure was applied for the production of C-doped TiO_2 nanotubes with thermal acetylene (C_2H_2) treatment. The pristine TiO_2 nanotubes were fabricated by using the anodization parameters that mentioned above (solution: aqueous 0.5 wt% HF electrolyte, anodization potential: 20 V, anodization time: 45 min). Then, the as-prepared (pristine) nanotubes were heated from room temperature to 500 °C in a quartz tube under N_2 flow. At a temperature of 500 °C, the nanotubes were treated under a continuous N_2 and C_2H_2 flux (1:1) for 10 min. Then, the treated TiO_2 nanotubes were cooled down to room temperature under a N_2 flow.

The morphologies of the un-doped and doped TiO_2 nanotubes were characterized by scanning electron microscopy (SEM, Philips XL 30S), and the elemental contents were determined by energy-dispersive X-ray analyses. The chemical compositions of the C-doped TiO_2 nanotubes were studied by X-ray photoelectron spectroscopy (XPS) analysis using a Phobus 150 Specs electron analyzer with a conventional X-ray source (Al Kα). To determine the thickness, the XPS signal of Ag $3d_{5/2}$ attenuation was used as a function of the time of metal exposure. The amount of loading was calculated using the formula developed by Tanuma, Powell, and Penn (the TPP formula) [38]. The atomic ratios of Ti, C and O were calculated using the density of each element. In addition, the crystallinity of the samples was established by X-ray diffraction (XRD, Philips 1820 X-ray diffractometer with Cu Kα radiation, $\lambda = 1.5418$ Å)

The hydrogen gas sensing properties of un-doped TiO_2 nanotubes and C-doped TiO_2 nanotubes that were fabricated by the chemical process were investigated at a temperature of 100 °C in a flow type home-made chamber. Silver paste was used to make direct electrical contact on the nanotube array with copper wires. Fig. 1 shows a schematic illustration of the

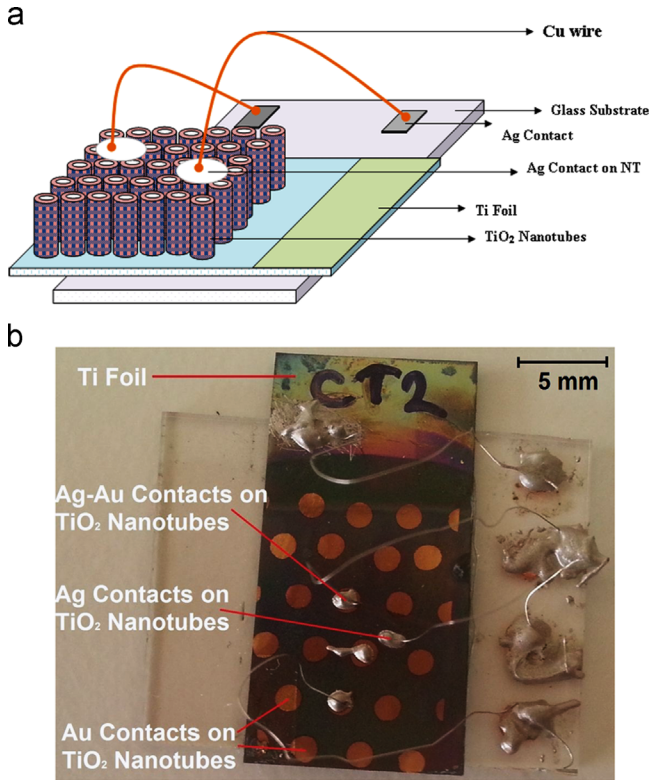

Fig. 1. Schematic illustration (a) and photograph (a) of the electrical contact of the TiO_2 nanotube sensor device.

electrical contact of the sensor device and a photograph of the device. Previously we used two spring-loaded platinum pads for electrical contacts [19]. It was difficult to apply the same pressure to the pads, and the electrical current between the pads varied with changing pressure. So, reproducible and repeatable sensor measurements with spring-loaded pads was dependent on pressure and was very difficult. In this study, silver epoxy was pasted directly on to TiO_2 nanotubes and on to Au thin film that was deposited on TiO_2 nanotubes with thickness of approximately 150 nm, in order to fix contacts, as seen in Fig. 1(b). But silver epoxy has two major problems; diffusion into the nanotube and contamination [18]. On the other hand, these problems do not prevent the comparison of the H_2 gas sensing properties of un-doped and C-doped TiO_2 nanotubes with silver paste contacts. A constant voltage was applied to un-doped and C-doped TiO_2 nanotube devices, and then the current of the devices was continuously measured using a Keithley 6517A Electrometer/High Resistance Meter and recorded using an IEEE 488 data acquisition system incorporated into a PC during the measurements. The sensor devices were exposed to a concentration of only 5000 ppm H_2 gas.

3. Results and discussion

Fig. 2 shows the top and cross sectional SEM images of un-doped TiO_2 nanotubes (a–c), and C-doped TiO_2 nanotubes that the C-doped nanotubes fabricated by using the chemical process (d–f). Tubular structures are clearly observed in all SEM images, but some parts of the C-doped TiO_2 nanotubes are covered with C (Fig. 2d and e). Similarly, the same images were obtained for C-doped TiO_2 nanotubes that were prepared with thermal acetylene (C_2H_2) treatment. The diameters of the un-doped and C-doped TiO_2 nanotubes are not homogeneous and vary between 40 nm and 110 nm, as seen in Fig. 2(b and e). The wall thickness and the tube length of the both un-doped and C-doped TiO_2 nanotubes are observed to be approximately 10 nm and above 300 nm, respectively (Fig. 2b, c and e, f). The formation mechanism of TiO_2 nanotubes fabricated by using an aqueous HF electrolyte with anodization is well known [1–4]. The rate of oxide formation and the rate of oxide dissolution are crucial to obtain the nanotubes. TiO_2 nanotubes are formed while both the formation and the dissolution rates are approximately equal.

Fig. 3(a) shows the EDX pattern of C-doped TiO_2 nanotubes prepared with the chemical process. C, Ti and O peaks are clearly seen from the EDX graph. Similarly, the same peaks are observed for C-doped TiO_2 nanotubes that were fabricated with thermal C_2H_2 treatment. Fig. 3(b) gives the XRD spectrum of un-doped and C-doped TiO_2 nanotubes for which the C doping is performed with the chemical process. The labels A, R and T represent the reflections from anatase crystallites, rutile crystallites, and the titanium substrate, respectively. Fig. 3(b) clearly shows that both the anatase and rutile phases of TiO_2 occur in the samples of C-doped and un-doped TiO_2 nanotubes. Previously, Varghese et al. found that the walls of the nanotubes adopt an anatase crystal structure and the rutile crystallite formation occurs at the interface between nanotubes for TiO_2 nanotubes annealed at 480 °C under dry air [39].

Fig. 4(a) shows the XPS spectrum of C-doped TiO_2 nanotubes that are prepared by using the chemical process. Ti2s, Ti2p, O1s and C1s peaks are clearly observed in the XPS analysis (Fig. 4a). Similar results are observed for C-doped TiO_2 nanotubes that are fabricated by using thermal C_2H_2 treatment. Fig. 4(b and c) shows the C1s XPS spectrum of C-doped TiO_2 nanotubes that are prepared by the chemical process and by the thermal C_2H_2 treatment. The peak areas of C1s are calculated using fitting procedure after the subtraction of background of the peak. The XPS analysis (Fig. 4b and c) of C-doped TiO_2 nanotubes that are synthesized with both the chemical process and thermal C_2H_2 treatment, shows three peaks at approximately 284.8 (C–C bond), 286.7 (C–O bond) and 289 (C═O bond) eV. The peaks at 284.8, 286.7 and 289 eV correspond to graphitized carbon, doped carbon in TiO_2 and carbonate species, respectively [33]. Fig. 4(b and c) clearly shows that the intensity of the graphitized carbon peak is higher than that of the doped carbon peak in TiO_2 and the carbonate peak. The carbon doping ratio is described as the ratio of doped carbon in TiO_2 to all of the carbon. The doping ratio is calculated to be 36% and 24% for C-doped TiO_2 nanotubes that are synthesized with the chemical process and the thermal C_2H_2 treatment, respectively. Thus, the chemical process is more efficient to dope TiO_2 nanotubes with a high doping ratio. Valentin and colleagues [40] described the possible positions for the presence of carbons atom in the

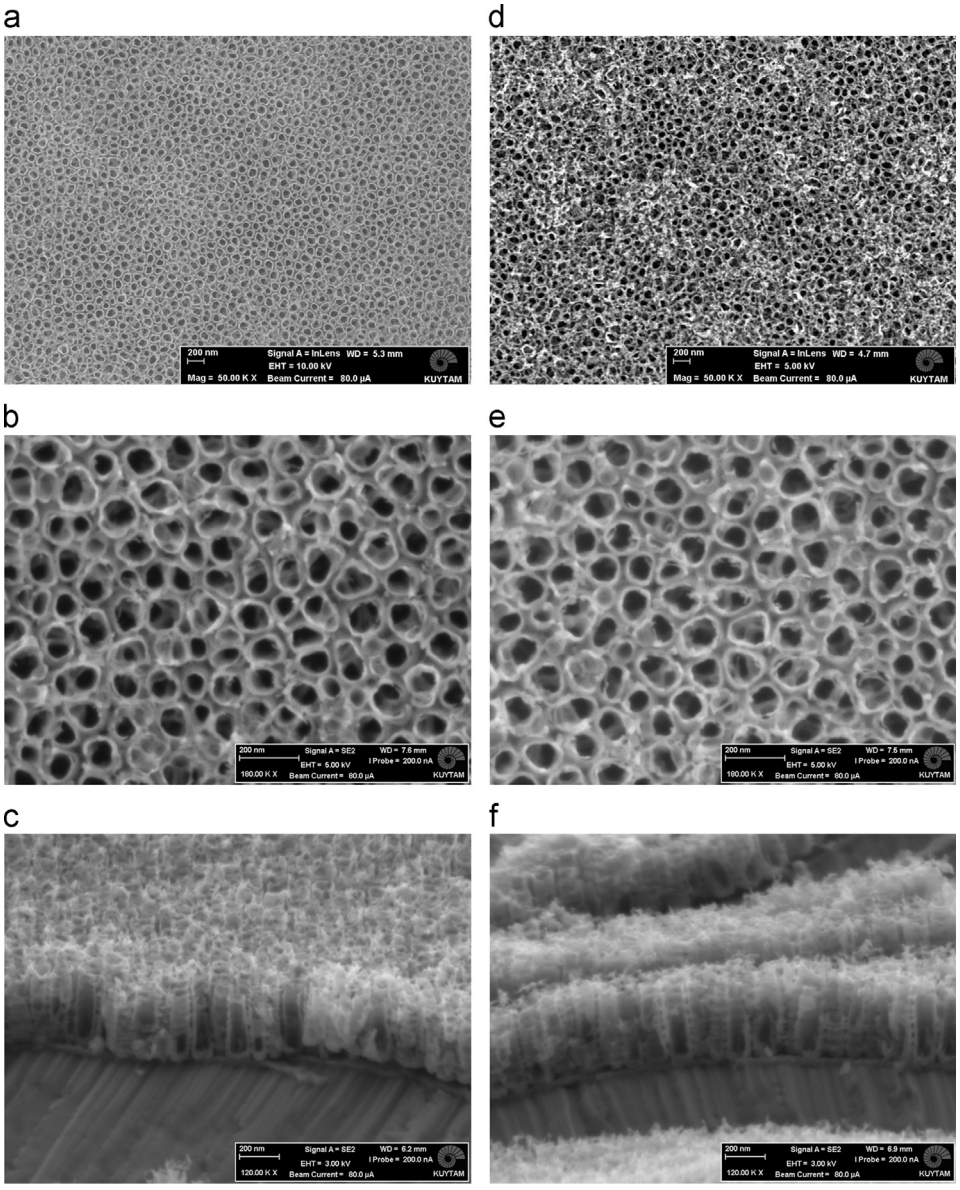

Fig. 2. Top and cross sectional SEM images of un-doped (with different magnifications (a) 50,000 × top image, (b) 180,000 × top image, and (c) 120,000 × cross sectional image), and of C-doped TiO_2 nanotubes fabricated by using the chemical process (with different magnifications (d) 50,000 × top image, (e) 180,000 × top image, and (f) 120,000 × cross sectional image).

anatase TiO_2: (i) the substitution of the oxygen lattice with carbon atoms, (ii) the replacement of Ti atoms with C atoms, and (iii) the stabilization of an interstitial position by carbon. In our case, the second situation could explain C doping process in TiO_2 nanotubes.

Fig. 5 shows the current versus time behavior of un-doped and C-doped TiO_2 nanotube sensors exposed to 5000 ppm H_2 at 100 °C. The base line currents of the un-doped and C-doped TiO_2 nanotubes were approximately 5 nA and 300 nA, respectively. Thus, the conductivity of the TiO_2 nanotubes increased with C doping, and this behavior can be mainly attributed to the reduced band gap of TiO_2 with C doping. The exposure to 5000 ppm H_2 caused an increase in current in both the un-doped and C-doped TiO_2 nanotubes, as shown in Fig. 5(a and b). The change in the electrical current of the C-doped TiO_2 nanotubes is low when the device is exposure to 5000 ppm H_2. The H_2 sensitivity of the un-doped TiO_2 nanotubes was higher than that of the C-doped TiO_2 nanotubes as shown in Fig. 5. Previously, the H_2 gas sensing properties of pristine TiO_2 nanotubes were investigated in the concentration range 100–5000 ppm and it was observed that limit of detection was lower than 100 ppm [19]. The low sensitivity of the C-doped TiO_2 nanotubes could be explained with high ratio of graphitized and carbonates carbons on the surface of TiO_2 nanotubes. On the other hand, the porosity of C-doped TiO_2 nanotube have little difference from un-doped TiO_2 nanotubes due to coverage of graphitized and carbonates carbons on some part of the surface as seen in cross sectional and top SEM images of them (Fig. 2a–f), but this

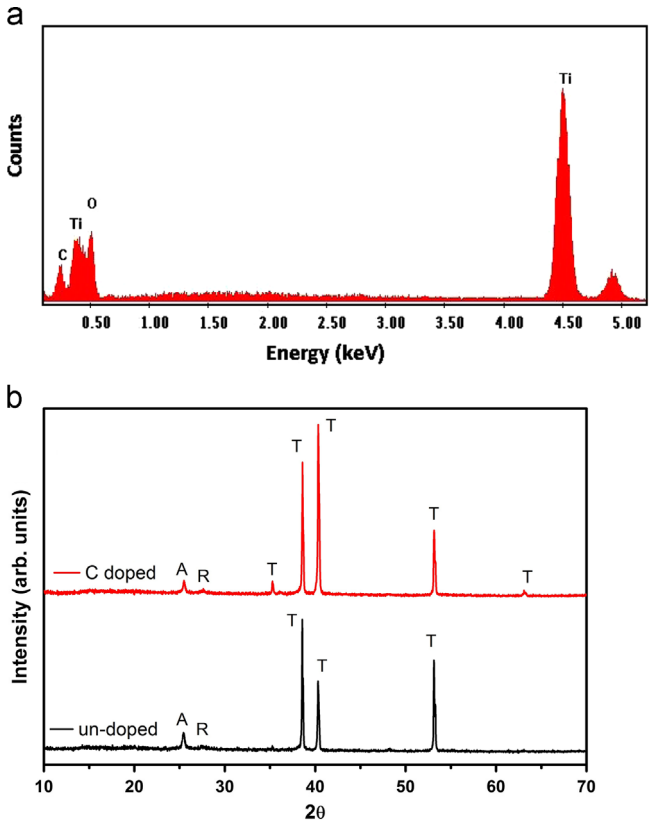

Fig. 3. EDX pattern of C-doped TiO_2 nanotubes prepared with the chemical process (a) and XRD spectrum of un-doped and C-doped TiO_2 nanotubes where the C doping was conducted with the chemical process (b).

low porosity difference could not be reason for low sensitivity. The ad/absorbtion of H_2 in TiO_2 nanotube causes dissociating H_2 molecules at the defects on the nanotube surface [18,41,42]. The major defects on the TiO_2 nanotube surface were oxygen vacancies because oxygen vacancies occur under high purity N_2 flow. The dissociated hydrogen could diffuse into the TiO_2 lattice and act as electron donors [18,41,42].

In general, there are two main factors to explain the increase in the current of TiO_2 when exposure to H_2. First, the chemisorbed oxygen on the surface of TiO_2 reacts with H_2 molecules and this leads to electron transfer from chemisorbed oxygen to TiO_2. For semiconductor gas sensors, this mechanism is the most well-known [43]. The second mechanism is based on Schottky barrier height between metal electrode and TiO_2. The dissolution of H_2 in to metal electrode causes a decrease in work function of the electrode and then Schottky barrier height at the interface between the electrode and TiO_2 decreases [44,45]. Egashira and co-workers investigated H_2 sensing properties of TiO_2 thin films that equipped with different kinds of metal electrodes and discussed sensing mechanism [44]. In our case, the increase in the current of both un-doped and C-doped TiO_2 nanotubes can be explained with decreasing Schottky barrier height at the interface between the electrode and the nanotubes. Nitrogen is used as carrier gas and the first sensing mechanism is not convenient for this case due to the deficiency of oxygen.

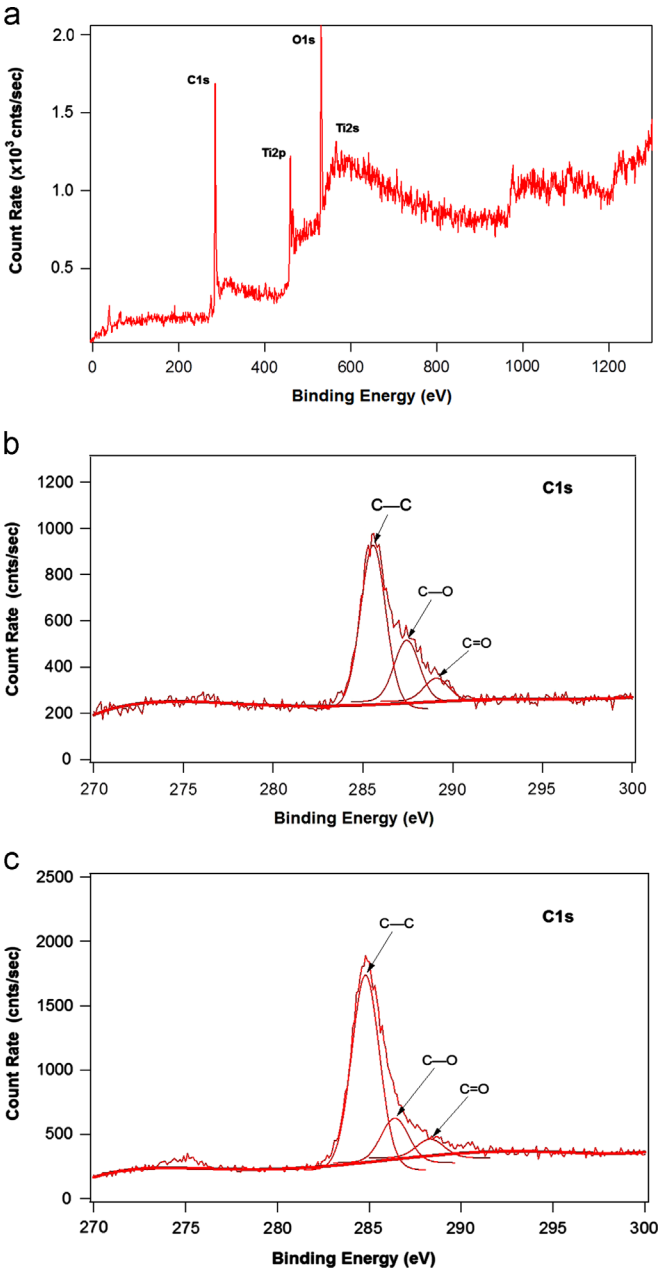

Fig. 4. XPS spectrum of C-doped TiO_2 nanotubes that were prepared by using the chemical process (a), C1s XPS spectrum of a TiO_2 nanotubes prepared by the chemical process (b) and thermal C_2H_2 treatment (c).

4. Conclusions

In summary, this study presented C-doped TiO_2 nanotubes fabricated with different methods. C doping into TiO_2 material was achieved by using a wet process and heat acetylene treatment. The high carbon doping ratio was observed for C-doped TiO_2 nanotubes prepared with the chemical process. The morphologies of the TiO_2 nanotubes changed with C doping for both doping processes because some parts of the tubular structure were covered with graphitized and carbonate carbon. The H_2 gas sensing properties of the un-doped and

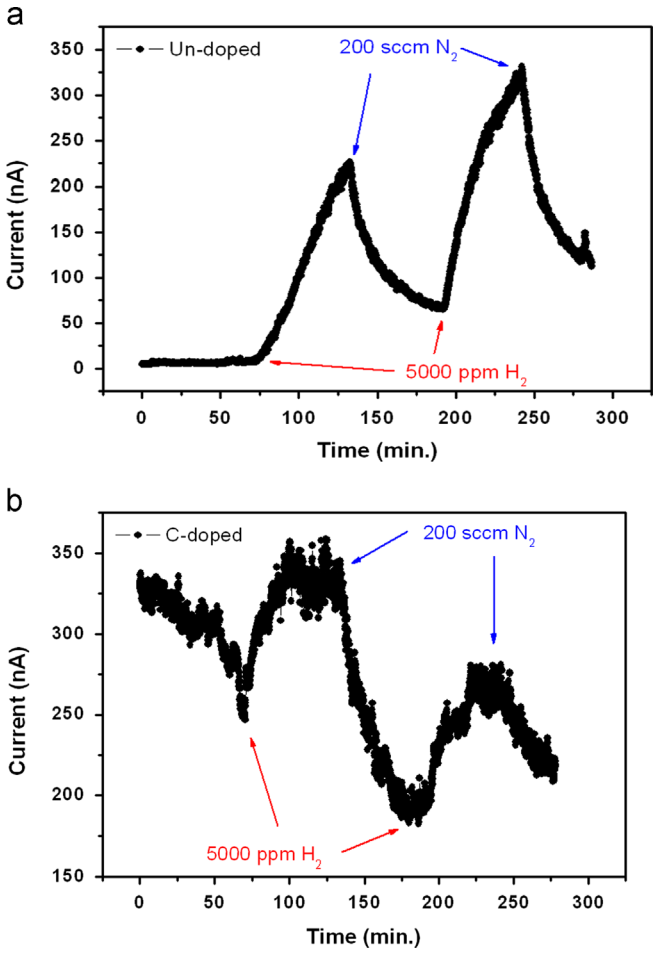

Fig. 5. Sensor response versus time for un-doped (a) and C-doped (b) TiO_2 nanotubes at 100 °C exposed to 5000 ppm H_2.

C-doped TiO_2 nanotubes was investigated at 100 °C, and the conductivity of the C-doped TiO_2 nanotubes was higher than that of the un-doped TiO_2 nanotubes. In addition, the carbon doping made the TiO_2 nanotubes less selective towards H_2 gas.

Acknowledgments

This work was partially funded by the Scientific and Technological Research Council of Turkey (TUBİTAK), Project number: 111M261. The authors thank KUYTAM and Dr. Barıs Yagci for SEM measurements.

References

[1] C.A. Grimes, G.K. Mor, TiO_2 Nanotube Arrays: Synthesis, Properties, and Applications, Springer Science & Business Media, LLC, New York http://dx.doi.org/10.1007/978-1-4419-0068-5.
[2] J.M. Macak, H. Tsuchiya, A. Ghicov, K. Yasuda, R. Hahn, S. Bauer, P. Schmuki, TiO_2 nanotubes: self-organized electrochemical formation, properties and applications, Current Opinion in Solid State and Materials Science 11 (2007) 3–18.
[3] G.K. Mor, O.K. Varghese, M. Paulose, K. Shankar, C.A. Grimes, A review on highly ordered, vertically oriented TiO_2 nanotube arrays: fabrication, material properties, and solar energy applications, Solar Energy Materials & Solar Cells 90 (2006) 2011–2075.
[4] C.A. Grimes, Synthesis and application of highly ordered arrays of TiO_2 nanotubes, Journal of Materials Chemistry 17 (2007) 1451–1457.
[5] Y.C. Nah, I. Paramasivam, P. Schmuki, Doped TiO_2 and TiO_2 nanotubes: synthesis and applications, ChemPhysChem 11 (2010) 2698–2713.
[6] P. Roy, S. Berger, P. Schmuki, TiO_2 nanotubes: synthesis and applications, Angewandte Chemie: International Edition 50 (2011) 2904–2939.
[7] V. Zwilling, M. Aucouturier, E. Darque-Ceretti, Anodic oxidation of titanium and TA6V alloy in chromic media. An electrochemical approach, Electrochimica Acta 45 (1999) 921–929.
[8] D. Gong, C.A. Grimes, O.K. Varghese, W.C. Hu, R.S. Singh, Z. Chen, E.C. Dickey, Titanium oxide nanotube arrays prepared by anodic oxidation, Journal of Materials Research 16 (2001) 3331–3334.
[9] J.H. Park, S. Kim, A.J. Bard, Novel carbon-doped TiO_2 nanotube arrays with high aspect ratios for efficient solar water splitting, Nano Letters 6 (2006) 24–28.
[10] H. Tokudome, M. Miyauchi, N-doped TiO_2 nanotube with visible light activity, Chemistry Letters 33 (2004) 1108–1109.
[11] N. Lu, X. Quan, J.Y. Li, S. Chen, H.T. Yu, G.H. Chen, Fabrication of boron-doped TiO_2 nanotube array electrode and investigation of its photoelectrochemical capability, Journal of Physical Chemistry C 111 (2007) 11836–11842.
[12] J.C. Xu, M. Lu, X.Y. Guo, H.L. Li, Zinc ions surface-doped titanium dioxide nanotubes and its photocatalysis activity for degradation of methyl orange in water, Journal of Molecular Catalysis A: Chemical 226 (2005) 123–127.
[13] A. Ghicov, B. Schmidt, J. Kunze, P. Schmuki, Photoresponse in the visible range from Cr doped TiO_2 nanotubes, Chemical Physics Letters 433 (2007) 323–326.
[14] D. Wu, Y.F. Chen, J. Liu, X.N. Zhao, A.D. Li, N.B. Ming, Co-doped titanate nanotubes, Applied Physics Letters 87 (2005).
[15] B.M. Wen, C.Y. Liu, Y. Liu, Bamboo-shaped Ag-doped TiO_2 nanowires with heterojunctions, Inorganic Chemistry 44 (2005) 6503–6505.
[16] Y.F. Tu, S.Y. Huang, J.P. Sang, X.W. Zou, Synthesis and photocatalytic properties of Sn-doped TiO_2 nanotube arrays, Journal of Alloys and Compounds 482 (2009) 382–387.
[17] L. Sun, J. Li, C.L. Wang, S.F. Li, H.B. Chen, C.J. Lin, An electrochemical strategy of doping Fe^{3+} into TiO_2 nanotube array films for enhancement in photocatalytic activity, Solar Energy Materials & Solar Cells 93 (2009) 1875–1880.
[18] O.K. Varghese, D.W. Gong, M. Paulose, K.G. Ong, C.A. Grimes, Hydrogen sensing using titania nanotubes, Sensors and Actuators B: Chemical 93 (2003) 338–344.
[19] E. Sennik, Z. Colak, N. Kilinc, Z.Z. Ozturk, Synthesis of highly-ordered TiO(2) nanotubes for a hydrogen sensor, International Journal of Hydrogen Energy 35 (2010) 4420–4427.
[20] G.K. Mor, O.K. Varghese, M. Paulose, K.G. Ong, C.A. Grimes, Fabrication of hydrogen sensors with transparent titanium oxide nanotube-array thin films as sensing elements, Thin Solid Films 496 (2006) 42–48.
[21] G.K. Mor, M.A. Carvalho, O.K. Varghese, M.V. Pishko, C.A. Grimes, A room-temperature TiO_2-nanotube hydrogen sensor able to self-clean photoactively from environmental contamination, Journal of Materials Research 19 (2004) 628–634.
[22] M. Paulose, O.K. Varghese, G.K. Mor, C.A. Grimes, K.G. Ong, Unprecedented ultra-high hydrogen gas sensitivity in undoped titania nanotubes, Nanotechnology 17 (2006) 398–402.
[23] O.K. Varghese, D.W. Gong, M. Paulose, K.G. Ong, E.C. Dickey, C.A. Grimes, Extreme changes in the electrical resistance of titania nanotubes with hydrogen exposure, Advanced Materials 15 (2003) 624–627.
[24] J. Lee, D.H. Kim, S.H. Hong, J.Y. Jho, A hydrogen gas sensor employing vertically aligned TiO_2 nanotube arrays prepared by template-assisted method, Sensors and Actuators B: Chemical 160 (2011) 1494–1498.
[25] H.G. Liu, D.Y. Ding, C.Q. Ning, Z.H. Li, Wide-range hydrogen sensing with Nb-doped TiO_2 nanotubes, Nanotechnology 23 (2012) 015502.
[26] Q. Wang, Y.Z. Pan, S.S. Huang, S.T. Ren, P. Li, J.J. Li, Resistive and capacitive response of nitrogen-doped TiO_2 nanotubes film humidity sensor, Nanotechnology 22 (2011) 025501.

[27] D. Mardare, N. Iftimie, M. Crisan, M. Raileanu, A. Yildiz, T. Coman, K. Pomoni, A. Vomvas, Electrical conduction mechanism and gas sensing properties of Pd-doped TiO_2 films, Journal of Non-Crystalline Solids 357 (2011) 1774–1779.
[28] Z.Y. Li, H.N. Zhang, W. Zheng, W. Wang, H.M. Huang, C. Wang, A.G. MacDiarmid, Y. Wei, Highly sensitive and stable humidity nanosensors based on LiCl doped TiO_2 electrospun nanofibers, Journal of the American Chemical Society 130 (2008) 5036–5037.
[29] J. Moon, J.A. Park, S.J. Lee, T. Zyung, I.D. Kim, Pd-doped TiO_2 nanofiber networks for gas sensor applications, Sensors and Actuators B: Chemical 149 (2010) 301–305.
[30] X.Y. Hu, T.C. Zhang, Z. Jin, J.X. Zhang, W. Xu, J. Yan, J.P. Zhang, L.D. Zhang, Y.C. Wu, Fabrication of carbon-modified TiO_2 nanotube arrays and their photocatalytic activity, Materials Letters 62 (2008) 4579–4581.
[31] R. Hahn, A. Ghicov, J. Salonen, V.-P. Lehto, P. Schmuki, Carbon doping of self-organized TiO_2 nanotube layers by thermal acetylene treatment, Nanotechnology 18 (2007) 105604.
[32] C. Xu, Y.A. Shaban, W.B. Ingler Jr., S.U.M. Khan, Nanotube enhanced photoresponse of carbon modified (CM)-*n*-TiO_2 for efficient water splitting, Solar Energy Materials & Solar Cells 91 (2007) 938–943.
[33] S. Sreekantan, K.A. Saharudin, Z. Lockman, T.W. Tzu, Fast-rate formation of TiO_2 nanotube arrays in an organic bath and their applications in photocatalysis, Nanotechnology 21 (2010) 365603.
[34] W. Krengvirat, S. Sreekantan, A.-F. Mohd. Noor, N. Negishi, S.Y. Oh, G. Kawamura, H. Muto, A. Matsuda, Carbon-incorporated TiO_2 photoelectrodes prepared via rapid-anodic oxidation for efficient visible-light hydrogen generation, International Journal of Hydrogen Energy 37 (2012) 10046–10056.
[35] L.-Q. Wang, C.-W. Wang, J.-B. Chen, R.-S. Guo, F. Zhou, W.-M. Liu, Electron field emission from the carbon-doped TiO_2 nanotube arrays, Thin Solid Films 519 (2011) 8173–8177.
[36] A. Mazare, I. Paramasivam, K. Lee, P. Schmuki, Improved water-splitting behaviour of flame annealed TiO_2 nanotubes, Electrochemistry Communications 13 (2011) 1030–1034.
[37] A. Mazare, I. Paramasivam, F. Schmidt-Stein, K. Lee, I. Demetrescu, P. Schmuki, Flame annealing effects on self-organized TiO_2 nanotubes, Electrochimica Acta 66 (2012) 12–21.
[38] S. Tanuma, C.J. Powell, D.R. Penn, Proposed formula for electron inelastic mean free paths based on calculations for 31 materials, Surface Science 192 (1987) L849–L857.
[39] O.K. Varghese, D.W. Gong, M. Paulose, C.A. Grimes, E.C. Dickey, Crystallization and high-temperature structural stability of titanium oxide nanotube arrays, Journal of Materials Research 18 (2003) 156–165.
[40] C.D. Valentin, G. Pacchioni, A. Selloni, Theory of carbon doping of titanium dioxide, Chemistry of Materials 17 (2005) 6656–6665.
[41] L.D. Birkefeld, A.M. Azad, S.A. Akbar, Carbon monoxide and hydrogen detection by anatase modification of titanium dioxide, Journal of the American Ceramic Society 75 (1992) 2964–2968.
[42] J.B. Bates, J.C. Wang, R.A. Perkins, Mechanisms for hydrogen diffusion in TiO_2, Physical Review B 19 (1979) 4130–4139.
[43] N. Yamazoe, N. Miura, Some basic aspects of semiconductor gas sensors, in: S. Yamauchi (Ed.), Chemical Sensor Technology, vol. 4, Kodansha-Elsevier, New York, 1992.
[44] Y. Shimizu, T. Hyodo, M. Egashira, H_2 sensing performance of anodically oxidized TiO_2 thin films equipped with Pd electrode, Sensors and Actuators B: Chemical 121 (2007) 219–230.
[45] H. Miyazaki, T. Hyodo, Y. Shimizu, M. Egashira, Hydrogen-sensing properties of anodically oxidized TiO_2 film sensors-effects of preparation and pretreatment conditions, Sensors and Actuators B: Chemical 108 (2005) 467–472.